

Cite this: *Chem. Sci.*, 2026, 17, 2990

## Enantioselective $C(sp^3)$ –H bond functionalization enabled by $Cp^xM(III)$ catalysis (M = Co, Rh, Ir)

Shu-Bin Mou,<sup>†,ab</sup> Mu-Peng Luo,<sup>†,b</sup> Feifei Fang,<sup>†,b</sup> Shi Cao,<sup>\*,b</sup> Dong Wu<sup>\*,a</sup> and Shou-Guo Wang<sup>†,b</sup>

Trivalent group 9 transition metals (Co, Rh, and Ir) bearing pentamethylcyclopentadienyl ( $Cp^x$ ) or structurally tailored  $Cp^x$  ligands have emerged as a transformative platform for asymmetric  $C(sp^3)$ –H functionalization. Despite significant progress in  $C(sp^2)$ –H activation, achieving site- and stereoselective transformation of  $C(sp^3)$ –H bonds remains a formidable synthetic challenge due to their intrinsic inertness, increased steric congestion and conformational flexibility. This review provides a comprehensive overview of recent advances in asymmetric  $C(sp^3)$ –H functionalization catalyzed by  $Cp^xM(III)$  (M = Co, Rh, Ir) complexes. Particular emphasis is placed on the evolution of chiral ligand frameworks, the strategic use of directing groups, and mechanistic insights into enantioselectivity. By integrating recent developments, this review highlights novel reactions and effective catalytic systems, clarifies remaining challenges, and outlines future research directions in this dynamic field. We anticipate that more novel  $Cp^xM(III)$ -catalyzed asymmetric  $C(sp^3)$ –H functionalization reactions will be developed and will find broad applicability in the near future.

Received 30th October 2025  
Accepted 19th January 2026

DOI: 10.1039/d5sc08394j  
[rsc.li/chemical-science](http://rsc.li/chemical-science)

## 1 Introduction

Over the past twenty years, tremendous progress in catalyst design, ligand innovation, and mechanistic elucidation has transformed transition metal-catalyzed C–H functionalization into a broadly applicable paradigm for complex molecule construction.<sup>1–13</sup> Transition metal-catalyzed C–H functionalization now provides a versatile and efficient platform for atom- and step-economical access to structurally diverse chiral molecules.<sup>14–19</sup> A wide range of transition metals have been successfully employed in asymmetric C–H activation, with notable contributions from palladium,<sup>20–23</sup> rhodium,<sup>24–27</sup> iridium,<sup>28–31</sup> cobalt<sup>32–35</sup> and others.<sup>36–39</sup> While the asymmetric functionalization of aromatic  $C(sp^2)$ –H bonds has advanced rapidly,<sup>40–42</sup> the direct enantioselective transformation of aliphatic  $C(sp^3)$ –H bonds remains a formidable challenge, owing to their lower acidity (higher  $pK_a$ ), low polarity, and intrinsic inertness. Direct, selective, and enantioselective  $C(sp^3)$ –H functionalization thus represents a streamlined strategy for installing stereogenic centers into simple hydrocarbons, enabling efficient construction of molecular complexity with profound implications for chiral molecule synthesis.

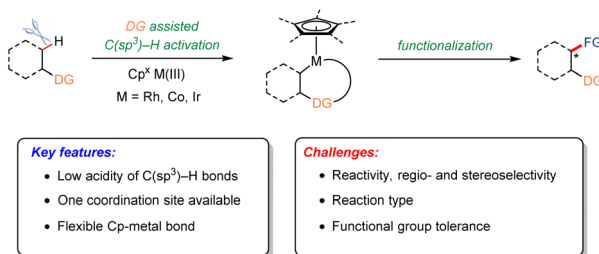
Pioneering contributions from the Ward and Rovis groups,<sup>43</sup> along with the Cramer group,<sup>44</sup> have played a central role in shaping chiral  $Cp^xRh(III)$ -catalyzed asymmetric C–H functionalization. A particularly transformative advance has been the development of chiral cyclopentadienyl ( $Cp^x$ ) metal complexes, especially  $Cp^xM(III)$  catalysts based on cobalt, rhodium, and iridium.<sup>45–48</sup> These catalysts combine exceptional reactivity with precise stereocontrol, enabling regio- and enantioselective formation of C–C and C–X bonds directly from inert aliphatic C–H sites, thereby eliminating the need for prefunctionalized substrates. The broad applicability of this approach—from pharmaceutical discovery to advanced material synthesis—further underscores its impact.<sup>26,49–52</sup> The rapid evolution of chiral  $Cp^xM(III)$  catalysts, novel reaction methodologies, and mechanistic understanding has collectively propelled the field forward.<sup>24,27,32</sup> These transformations typically proceed through substrate coordination to the metal center, selective C–H bond cleavage to generate an alkyl–metal intermediate, and subsequent functionalization (Scheme 1). The modular steric and electronic tunability of  $Cp^x$  ligands provides fine control of both regio- and enantioselectivity, enabling the direct synthesis of enantioenriched molecules with high levels of asymmetric induction. Mechanistic studies have further revealed the critical roles of metal–ligand cooperativity, coordination geometry, and substrate stereoelectronics in governing reactivity and selectivity. As these catalytic systems mature, they are poised to become indispensable tools for stereoselective synthesis, transforming simple aliphatic hydrocarbons into architecturally sophisticated chiral molecules.

<sup>a</sup>Computer Aided Drug Discovery Center, Zhuhai Institute of Advanced Technology, Chinese Academy of Sciences, Zhuhai 519003, P. R. China. E-mail: wudong@ziat.ac.cn

<sup>b</sup>College of Chemistry and Environmental Engineering, Shenzhen University, Shenzhen 518060, P. R. China. E-mail: shichaorganic@szu.edu.cn; shouguo.wang@szu.edu.cn

† These authors contributed equally.





**Scheme 1**  $\text{Cp}^x\text{M}(\text{III})$  ( $\text{M} = \text{Co, Rh, Ir}$ )-catalyzed asymmetric  $\text{C}(\text{sp}^3)\text{-H}$  functionalization.

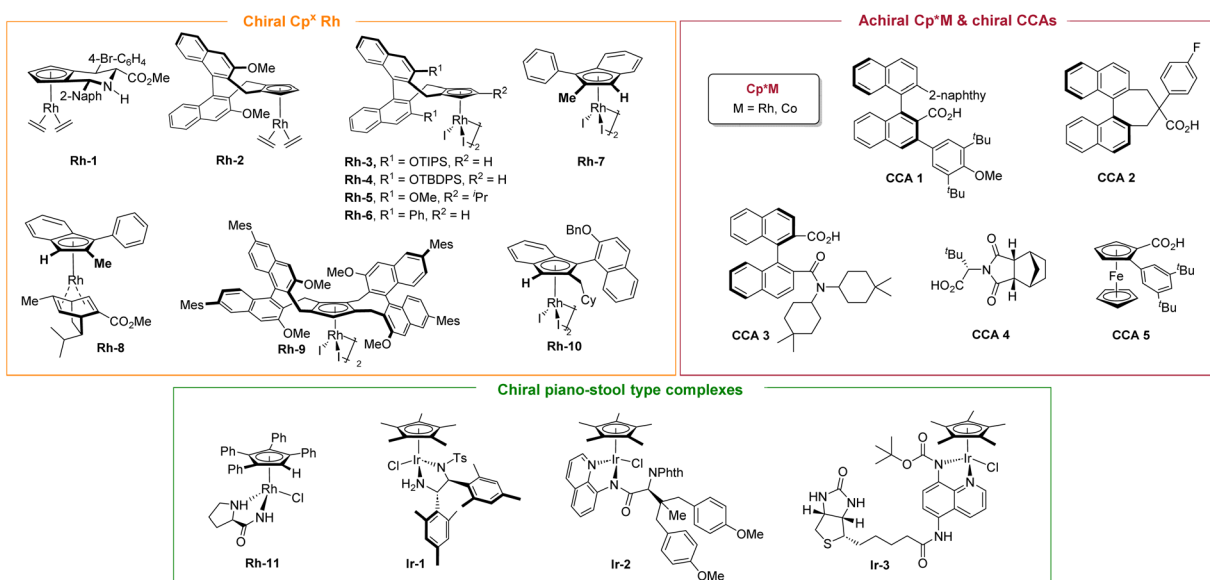
Enantiocontrol in  $\text{C}(\text{sp}^3)\text{-H}$  functionalization has primarily been achieved through three complementary strategies that exploit distinct chiral sources to deliver high levels of stereo-selectivity (Scheme 2). The most extensively developed approach employs chiral cyclopentadienyl ( $\text{Cp}$  or  $\text{Cp}^x$ ) metal(III) complexes, which provide a robust platform for  $\text{C}(\text{sp}^3)\text{-H}$  activation.<sup>25,53</sup> By tailoring the steric and electronic properties of the  $\text{Cp}$  framework, a highly organized chiral environment is established around the metal center, enabling precise enantioselective bond formation. A second strategy uses achiral  $\text{Cp}^x\text{M}(\text{III})$  complexes in combination with chiral carboxylic acid (CCA) additives.<sup>49</sup> In this co-catalytic system, the CCA functions as a transient chiral ligand or proton shuttle during the concerted metalation-deprotonation (CMD) step, transferring stereochemical information through a dynamic anion–metal interaction. This approach is operationally simple, highly modular, and particularly effective for challenging substrates. A third, conceptually distinct avenue employs chiral piano-stool complexes that operate *via* outer-sphere mechanisms.<sup>54–56</sup> Here, stereocontrol arises not from direct metal–substrate bonding but from non-covalent interactions—such as hydrogen bonding,  $\pi$ – $\pi$  stacking, and hydrophobic effects—that selectively stabilize one transition state over another. Together, these

strategies illustrate the conceptual breadth and growing sophistication of asymmetric  $\text{C}(\text{sp}^3)\text{-H}$  functionalization. Innovations in ligand design, co-catalysis, and mechanistic understanding continue to expand the range of achievable transformations. The ability to convert simple hydrocarbons directly into complex chiral architectures underscores the growing importance of this field in modern synthesis and highlights the need for a dedicated review.

Previous surveys of transition metal-catalyzed  $\text{C-H}$  activation have largely emphasized  $\text{C}(\text{sp}^2)\text{-H}$  functionalization or provided broad overviews across multiple catalytic systems. In contrast, this article focuses specifically on asymmetric  $\text{C}(\text{sp}^3)\text{-H}$  functionalization mediated by  $\text{Cp}^x\text{M}(\text{III})$  catalysts. The discussion is organized by transition metal (Co, Rh, Ir), with emphasis on ligand design, mechanistic paradigms, and emerging synthetic applications. By consolidating recent advances and highlighting key challenges, this review aims to capture the state of the art and provide a framework for future developments in this rapidly advancing field.

## 2 $\text{Cp}^x\text{Rh}(\text{III})$ -catalyzed asymmetric $\text{C}(\text{sp}^3)\text{-H}$ functionalization

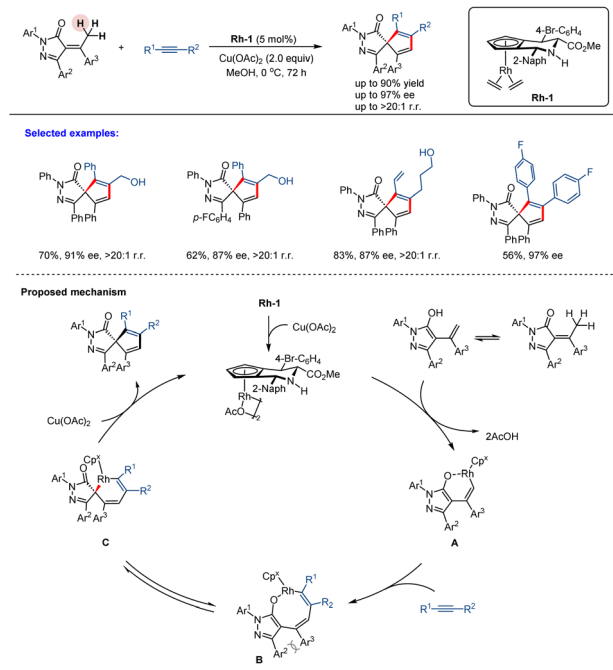
In 2019, Waldmann and co-workers reported an enantio-selective annulation of  $\alpha$ -arylidene pyrazolones with alkynes *via* a formal  $\text{C}(\text{sp}^3)\text{-H}$  activation, catalyzed by a piperidine-fused chiral  $\text{Cp}^x\text{Rh}(\text{III})$  catalyst **Rh-1** (Scheme 3).<sup>57</sup> This method provided access to a diverse array of spiropyrazolones in high yields and excellent enantioselectivities (up to 97% ee). Mechanistically, tautomerization of the pyrazolone generates its enol form, which undergoes formal  $\text{C}(\text{sp}^3)\text{-H}$  activation to form a six-membered rhodacycle intermediate **A**. The subsequent migratory insertion is regioselective for the alkyne carbon adjacent to the alkyl substituent, leading to an eight-membered rhodacycle



**Scheme 2** Representative chiral  $\text{Cp}^x\text{M}(\text{III})$  ( $\text{M} = \text{Co, Rh, Ir}$ ) catalytic system covered in this review.



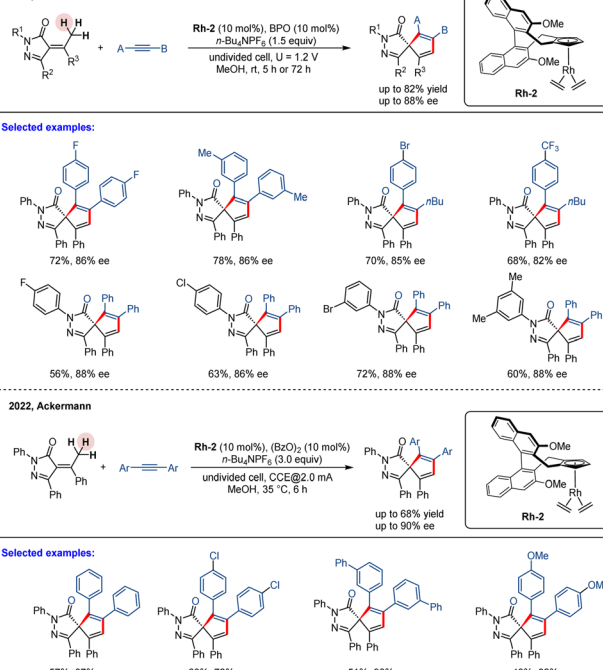
2019, Waldmann and Antonchick

Scheme 3 Rh(III)-catalyzed asymmetric annulation of  $\alpha$ -arylidene pyrazolones via  $C(sp^3)$ -H activation.

intermediate **B**. Due to steric interactions between the  $Ar^2$  and  $Ar^3$  substituents, intermediate **B** isomerizes to intermediate **C**, which then undergoes reductive elimination to furnish the spiropyrazolone as a single regioisomer. The catalytic cycle is completed by reoxidation of Rh(I) to Rh(III) using  $Cu(OAc)_2$  as an oxidant. However,  $O_2$  inhibited the catalysis under otherwise identical conditions, suggesting it acts as a potent catalyst poison, likely by quenching intermediates or causing oxidative decomposition. This transformation is applicable to the late-stage diversification of chiral pharmaceuticals and natural products. The process was also demonstrated to proceed in a catalyst-directed manner with high diastereoselectivity ( $>95:5$  d.r.), affording a single diastereoisomer. Beyond their synthetic utility, the spiropyrazolones obtained through this method exhibit biological activity, showing preliminary promise as a new class of Hedgehog pathway inhibitors.

While stoichiometric oxidants remain a common necessity in catalysis, electric current offers a clean and sustainable alternative. This powerful strategy has recently been extended to metal-catalyzed enantioselective C-H functionalization, merging the principles of green chemistry with asymmetric catalysis to achieve challenging transformations under mild conditions.<sup>58</sup> In 2021, Mei, You, and co-workers reported a highly efficient, electrochemically tuned rhodium-catalyzed system for the enantioselective formal  $C(sp^3)$ -H annulation of pyrazolones with alkynes (Scheme 4).<sup>59</sup> This operationally simple method, conducted in an undivided cell at room temperature, efficiently furnished a diverse array of spiro-pyrazolones in high yields (up to 82%) and with good enantiocontrol (up to 88% ee). The reaction employs a chiral BINOL-derived rhodium complex (**Rh-2**) as a precatalyst and benzoyl

2021, Mei and You

Scheme 4 Rh(III)-catalyzed enantioselective electrochemical  $C(sp^3)$ -H activation.

peroxide (BPO) as a key oxidative additive, with a reticulated vitreous carbon (RVC) anode and platinum cathode completing the electrochemical system (Scheme 4). In contrast to Waldmann's work, the reaction proceeds *via* a similar pathway; however, in this system, the  $Cp^xRh(III)$  catalyst is regenerated through anodic oxidation, eliminating the need for a stoichiometric chemical oxidant. Notably, this method accommodates unsymmetrical alkylarylacetylenes, which undergo smooth spiroannulation to deliver products with outstanding regiocontrol ( $>95:5$  r.r.) and enantioselectivities.

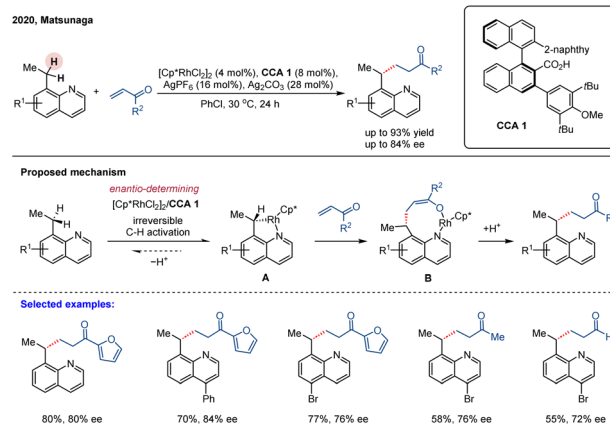
Almost simultaneously, a similar study was disclosed by Ackermann and co-workers.<sup>60</sup> They reported an electrooxidative, enantioselective rhodium(III)-catalyzed [3 + 2] spiroannulation of pyrazolones with alkynes *via*  $C(sp^3)$ -H activation, using a chiral BINOL-derived rhodium complex (**Rh-2**) as a precatalyst (Scheme 4). This protocol employs electricity as a green oxidant under mild conditions, replacing stoichiometric chemical oxidants and generating molecular hydrogen ( $H_2$ ) as the sole byproduct. Using a simple undivided cell, this approach provided direct access to an array of spirocyclic spiro-pyrazolones in moderate yield and with high enantioselectivities (up to 90% ee). Although this catalytic system exhibits good functional group tolerance with symmetrical alkynes, unsymmetrically substituted alkynes were found to be unreactive under these conditions. Note that by successfully merging electrochemistry with asymmetric catalysis, these developments provide powerful new strategies for C-H functionalization and complex molecule synthesis.

Although chiral  $Cp^xRh(III)$  complexes have garnered significant attention as privileged catalysts for asymmetric C-H functionalization, achiral  $Cp^xRh(III)$ /chiral carboxylic acid (CCA)



cooperative systems have emerged as a powerful and complementary strategy.<sup>49</sup> In 2019, Matsunaga and colleagues reported a catalytic enantioselective directed amidation of methylene C(sp<sup>3</sup>)-H bonds in 8-alkylquinolines with dioxazolones as the amidation reagent under a Cp\*Rh(III)/chiral carboxylic acid hybrid catalytic system (Scheme 5).<sup>61</sup> The quinoline moiety served as a directing group to enable chemoselective C(sp<sup>3</sup>)-H activation, while the chiral carboxylic acid ligand controlled the enantioselective cleavage of the methylene C(sp<sup>3</sup>)-H bonds, leading to the stereoselective formation of a new C-N bond at the stereogenic center. This method provided direct and efficient access to enantioenriched amide derivatives under mild reaction conditions, exhibiting both high reaction efficacy and enantioselectivities (up to 88% ee). In this study, the authors conducted a systematic evaluation of various chiral carboxylic acids (CCAs) and identified binaphthyl-derived analogues as the most effective ligand class, initially achieving an enantiomeric ratio (er) of 68:32. Further structural refinement of the binaphthyl scaffold demonstrated that introducing *ortho*-substituents on the aryl group adjacent to the carboxylic acid significantly improved stereochemical control. Notably, employing CCA 1—featuring a 3,5-di-*tert*-butyl-4-methoxyphenyl substituent—under optimized conditions afforded the target  $\gamma$ -lactam product in 83% yield with 92:8 er (Scheme 5). The practical value of this methodology was underscored by the efficient, modular synthesis of the binaphthyl-based CCAs from commercially available BINOL in five steps. This work demonstrates the synergistic combination of achiral Cp\*Rh(III) and readily tunable chiral carboxylic acids as an efficient asymmetric catalytic platform for the challenging enantioselective C(sp<sup>3</sup>)-H functionalization.

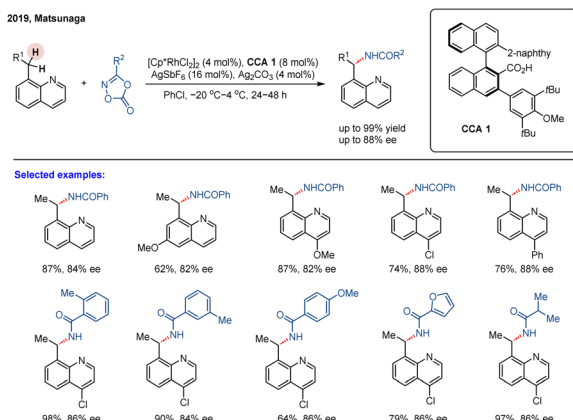
As an intriguing extension of their work, Matsunaga group disclosed an asymmetric alkylation of 8-ethylquinolines with  $\alpha,\beta$ -unsaturated carbonyl compounds by integrating C(sp<sup>3</sup>)-H activation with subsequent C-C bond formation (Scheme 6).<sup>62</sup> The reaction proceeded under mild conditions with good functional group tolerance but afforded modest enantioselectivities (74–84% ee). The chiral acid scaffold is the key determinant of enantioselectivity in this system; therefore, the



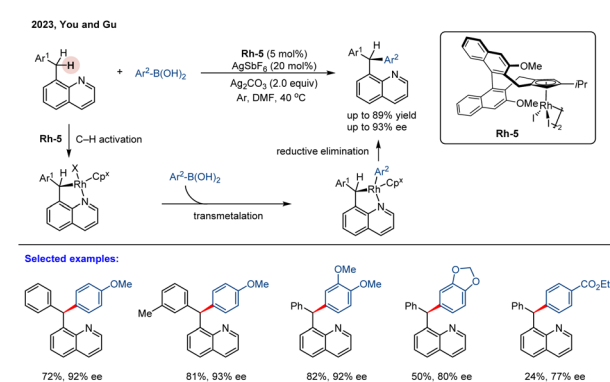
Scheme 6 Rh(III)/CCA catalyzed enantioselective C(sp<sup>3</sup>)-H alkylation of 8-ethylquinolines.

development of next-generation ligands constitutes the most viable path to achieving higher levels of enantiocontrol. H/D exchange experiments indicated that the C-H activation step is irreversible. Meanwhile, 18% deuterium incorporation was detected at the  $\alpha$ -position of the carbonyl group in the product, suggesting the formation of an enolate intermediate. Overall, the mechanism studies indicate that CCA 1 mediates the enantioselective C-H activation step, thereby irreversibly generating metallacycle A in this catalytic system. Subsequent insertion of the enone and tautomerization of the resulting enol generates a nine-membered rhodacycle intermediate B. This intermediate then undergoes further protonation by the proton generated in the C-H activation step, thereby furnishing the final alkylated product and regenerating the active catalyst. Notably, substrates with 8-propyl and 8-pentyl substituents exhibited significantly lower reactivity under the standard conditions.

In 2023, You and co-workers reported an asymmetric benzylic C(sp<sup>3</sup>)-H arylation of 8-benzylquinolines with arylboronic acids (Scheme 7).<sup>63</sup> Employing a BINOL-derived chiral cyclopentadienyl rhodium complex Rh-5 as the catalyst, the benzylic C(sp<sup>3</sup>)-H arylation proceeded efficiently to produce a series of enantioenriched triarylmethanes in high yields (up to



Scheme 5 Enantioselective C(sp<sup>3</sup>)-H amidation of 8-alkylquinolines enabled by Cp\*Rh(III)/CCA catalysis.



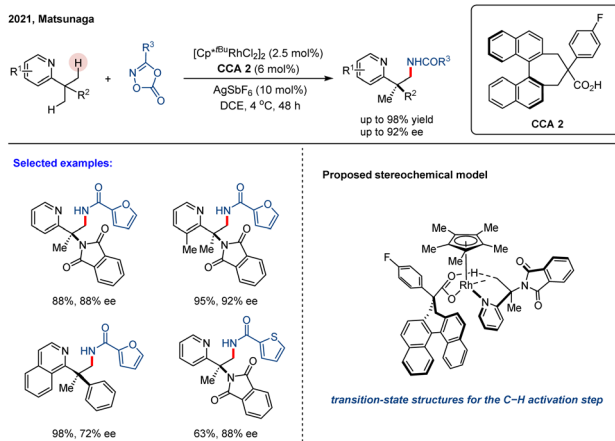
Scheme 7 Rh(III)-catalyzed asymmetric arylation of 8-benzylquinolines with arylboronic acids.



89%) with outstanding enantioselectivities (up to 93% ee). The catalytic system demonstrates broad substrate scope and excellent functional group tolerance under mild reaction conditions, providing a practical approach to valuable chiral triarylmethane scaffolds. The reaction commences with the irreversible, quinoline-directed C–H activation, forming a key rhodacyclic intermediate. This intermediate then undergoes transmetalation with the arylboronic acid, followed by reductive elimination to deliver the final product. The mechanistic study results demonstrate that the C–H activation step operates through an irreversible and enantio-determining pathway.

In 2021, Matsunaga and co-workers developed a series of pseudo- $C_2$ -symmetric chiral carboxylic acids (CCAs) based on a binaphthyl backbone, which were successfully applied in the enantioselective  $C(sp^3)$ –H amidation of *gem*-dimethyl-substituted pyridine substrates (Scheme 8).<sup>64</sup> The combination of sterically hindered  $Cp^{*t\text{Bu}}\text{Rh}(\text{III})$  and an optimal CCA 2 exhibits high enantiocontrol in this desymmetrization process (up to 92% ee). This transformation successfully accommodated both *N*-methylbenzimidazoles and isoquinoline derivatives, delivering the desired products in high yields and enantioselectivities. In contrast to  $C_1$ -symmetric analogues, these pseudo- $C_2$ -symmetric CCAs possess restricted conformational flexibility arising from the 2,2'-quaternary carbon bridge in their binaphthyl framework, thereby enforcing a well-defined chiral environment. Notably, a library of tunable chiral carboxylic acid ligands could be synthesized in two or three steps, which would enable rapid optimization of other valuable reactions. Mechanistic insights derived from DFT calculations and conformational analysis suggested that noncovalent interactions, such as  $\pi$ – $\pi$  stacking or C–H– $\pi$  interactions between the naphthyl moiety of CCA 2 and the pyridine moiety, played a decisive role in the enantio-induction process (Scheme 8).

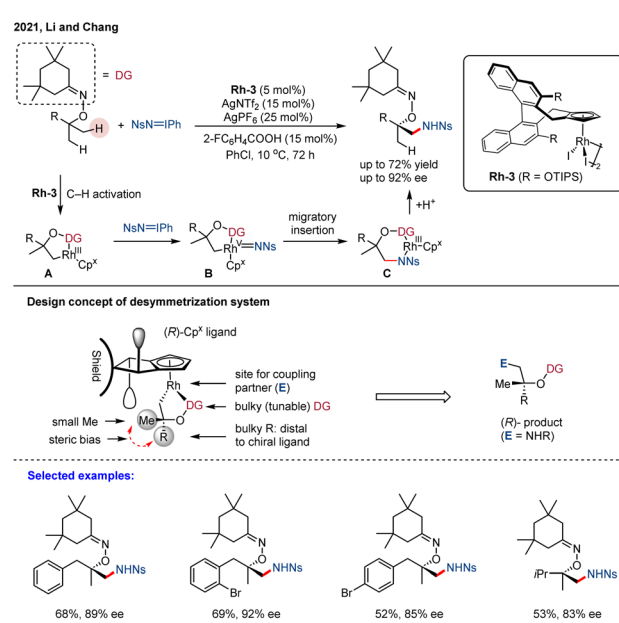
In 2021, Li and co-workers reported an enantioselective  $Cp^*\text{Rh}(\text{III})$ -catalyzed amination of geminal dimethyl containing compounds, affording a series of  $\beta$ -amino alcohol derivatives in up to 92% ee (Scheme 9).<sup>65</sup> The enantioselective  $C(sp^3)$ –H amination was accessed by a desymmetrization strategy using iminiodinane as the N-source. Other N-sources such as  $Ts\text{N}_3$  or



**Scheme 8** Rh(III)/CCA-catalyzed enantioselective  $C(sp^3)$ –H amidation of 2-alkylpyridines.

dioxazolone were proven inactive in this transformation. While this catalytic system tolerates a diverse range of substrates, the enantioselectivity is critically modulated by the presence of an appropriate oxime directing group, a bulkier *R* substituent (such as *t*Bu-, Ar-, Bn-), and a judiciously selected aminating reagent. Mechanistic analysis indicates that steric repulsion between the ligand and substrate governs both substrate orientation and transition state stabilization, leading to the high enantioselectivity. Using Rh-3 as a catalyst, a bulky directing group (oxime) was employed to assist stereodetermining C–H activation by spatially biasing one methyl group closer to the chiral pocket of the catalyst, thereby forming a rhodacycle intermediate A. Subsequently, Rh<sup>V</sup>–nitrene formation (intermediate B) and migratory insertion into the nitrene generates intermediate C, which is followed by protonolysis to afford the final amination product. Studies involving H/D exchange and the kinetic isotope effect (KIE) reveal that methyl C–H activation is an irreversible and turnover-limiting step. This work highlights both the potential and the challenges of achieving high stereocontrol in simple hydrocarbon motifs.

In 2024, Liu and co-workers reported a Rh(III)-catalyzed enantioselective  $C(sp^3)$ –H heteroarylation of *gem*-dimethyl-substituted pyridine derivatives *via* a desymmetrization strategy.<sup>66</sup> This reaction employs an *in situ*-generated arylating reagent, formed by the nucleophilic cyclization of an *o*-aminoaryl alkyne. Using Rh-4 as a catalyst, this catalytic system achieves outstanding enantiocontrol (up to 92% ee) in the synthesis of chiral indoles with all-carbon quaternary stereocenters (Scheme 10). The reaction was proposed to be initiated by carboxylate assisted methyl C–H activation of pyridine to afford rhodacycle intermediate A. Then, intermediate A undergoes coordination with *ortho*-aminoaryl alkyne (intermediate B) and *in situ* nucleophilic cyclization to generate Rh-aryl species D



**Scheme 9** Rh(III)-catalyzed enantioselective  $C(sp^3)$ –H amination of *gem*-dimethyl groups.

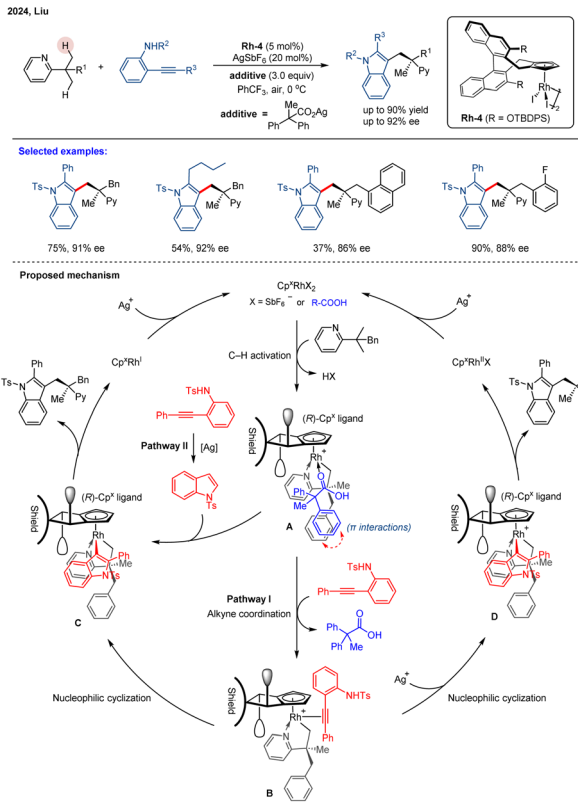


(pathway I). Then, the chiral indole product and a Rh(i) species are released by reductive elimination. Finally, the active Rh(III)-catalyst is regenerated by the oxidation of Ag(I). The *in situ* nucleophilic cyclization and indole formation mediated by Rh(III) species and subsequent Rh-aryl bond formation proved essential for high reaction efficiency. Alternatively, the chiral product could be afforded *via* pathway II, involving a NTs-indole intermediate generated from an *ortho*-aminoaryl alkyne through Ag-assisted nucleophilic cyclization. However, this pathway proved to be significantly less efficient. Notably, the ((2,2-diphenylpropanoyl)oxy)silver additive was crucial for achieving high stereoselectivity. Unlike previous approaches that relied on steric differentiation from bulky directing groups, stereocontrol in this system is achieved through a synergistic mechanism. Mechanistic and DFT studies reveal that the large side arm of the chiral  $\text{Cp}^x$  ligand (bearing an -OTBDPS group), combined with non-covalent interactions—such as C–H $\cdots$  $\pi$  and lone pair $\cdots$  $\pi$  (LP $\cdots$  $\pi$ ) interactions between the carboxylate additive and the substrate—plays key roles in orienting the substrate within the chiral pocket of the catalyst.

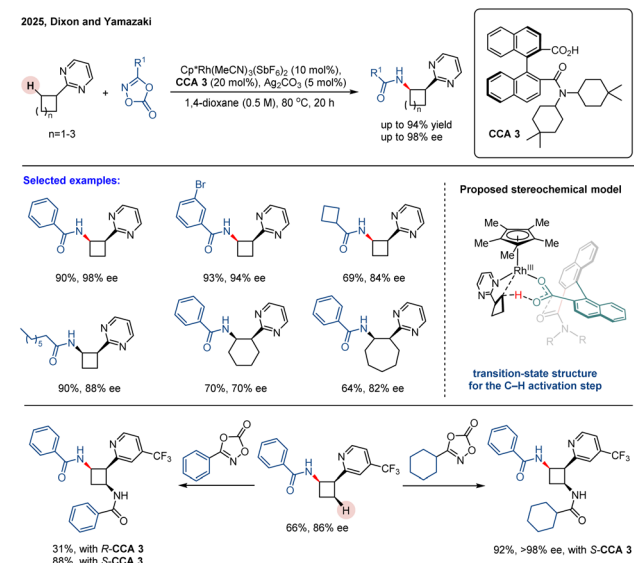
The unique properties of the saturated cyclobutane ring make it a valuable structural motif in pharmaceutical chemistry. Recently, Dixon<sup>67</sup> and co-workers reported an enantioselective amidation of cyclobutanes bearing a coordinating azine-type directing group, catalyzed by an electron-deficient  $\text{Cp}^x\text{Rh}(\text{III})$  complex in combination with a novel axially chiral carboxylic acid CCA 3 (Scheme 11).<sup>67</sup> A broad range of substituted

dioxazolones were compatible with this transformation, affording the desired products in moderate to excellent enantioselectivities (up to 98% ee) and yields (up to 94%). This method was also applied to homologous cyclohexyl and cycloheptyl substrates, providing the corresponding products in moderate yields with good enantioselectivities. In contrast, the catalytic system exhibited much diminished reactivity with cyclopentyl and cyclopropyl analogs. Furthermore, an enantio-enriched bis-amidated pyridylcyclobutane was accessible following minor optimization of the reaction parameters. The proposed mechanism begins with the coordination of the pyrimidine and chiral acid co-catalyst to the  $\text{Cp}^*\text{Rh}(\text{III})$  center, followed by activation of the adjacent cyclobutyl C–H bond *via* an ambiphilic metal–ligand activation/concerted metalation–deprotonation (AMLA/CMD) mechanism. The kinetic isotope effect study showed that C–H bond cleavage occurs in the rate-determining step. Combining mechanistic studies with DFT calculations, the authors elucidated the origin of the enantioselectivity. Notably, the novel axially chiral carboxylic acid CCA 3, designed based on prior work by the Shi group,<sup>68</sup> proved crucial for achieving high enantiocontrol. The fine-tuned catalytic system achieves high selectivity by stabilizing the ligand conformation through non-covalent interactions. The resulting conformation creates steric repulsion with the substrate, which induces ring strain in the transition state that leads to the minor enantiomer, thereby suppressing its formation.

Despite the success of chiral  $\text{Cp}^x\text{M}(\text{III})$  complexes in asymmetric catalysis, their enantiocontrol typically relies on steric shielding provided by judicious ligand design. In 2020, Blakey and co-workers introduced a novel class of planar chiral indenyl–rhodium(III) complexes **Rh-7** that achieved enantiocontrol by exploiting electronic asymmetry rather than conventional steric bias.<sup>69</sup> Remarkably, these chiral indenyl–Rh catalysts could be synthesized in only four steps from commercially available starting materials. Importantly, chiral



Scheme 10 Rh(III)-catalyzed enantioselective  $\text{C}(\text{sp}^3)\text{–H}$  heteroarylation of gem-dimethyl groups.



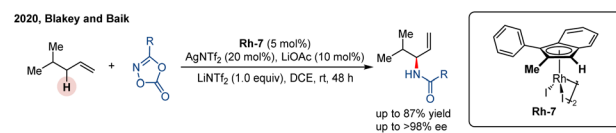
Scheme 11 Rh(III)/CCA-catalyzed asymmetric  $\text{C}(\text{sp}^3)\text{–H}$  amidation of azine-linked cyclobutanes.



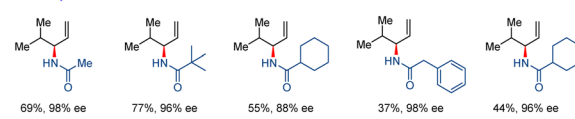
HPLC purification was required to obtain the enantiopure complexes (Scheme 12). They further applied this catalytic system to the asymmetric allylic C–H amidation of unactivated terminal olefins using dioxazolones as effective amidating reagents, affording a wide array of enantioenriched allylic amides with high yields (up to 87%), excellent regioselectivity (up to >20:1 r.r.), and outstanding enantioselectivities (up to >98% ee). The catalytic system was less reactive with internal olefin substrates, although it maintained high enantioselectivity. The proposed catalytic cycle is illustrated in Scheme 13. The reaction begins with the generation of a coordinatively unsaturated cationic indenyl–Rh complex **A** via activation of the dimeric precatalyst by  $\text{AgNTf}_2$  and  $\text{LiOAc}$ . Subsequent coordination of the olefin produces intermediate **B**, which undergoes rate- and enantio-determining allylic C–H cleavage to form a  $\pi$ -allyl complex **C**. Coordination of the dioxazolone and loss of  $\text{CO}_2$  yields a reactive nitrene intermediate **D**, which undergoes regio-determining C–N bond formation to generate complex **E**. Finally, protodemetalation of **E** furnishes the desired allylic amide product and regenerates the active species **A**. Crystallographic analyses and computational studies revealed that both regio- and enantioselectivity are governed by a synergistic combination of electronic asymmetry and steric interactions imparted by the indenyl ligand framework.

Given the persistent challenge of resolving planar chiral  $\text{Cp}^x\text{Rh}(\text{III})$  complexes, Wang and co-workers developed a practical and robust chiral resolution strategy.<sup>70</sup> In this case, the chiral precursor  $[\text{Rh}(\text{chiral diene})\text{OAc}]_2$  was synthesized in three steps from the readily available  $(-)\alpha$ -phellandrene. Subsequent ligand exchange with various  $\text{Cp}^x$  ligands afforded a pair of air-stable  $\text{Cp}^x\text{Rh}(\text{chiral diene})$  diastereomers, which could be readily separated by silica gel flash chromatography (Scheme 14). This strategy enables the efficient and scalable preparation of a diverse set of tetrasubstituted planar chiral indenyl ligands without the need for extensive chiral HPLC purification or auxiliary-based resolution. The utility of these chiral indenyl–Rh(III) complexes was demonstrated across a range of asymmetric C–H functionalization reactions, notably including the allylic C–H amidation of an unactivated terminal olefin with excellent reactivity and enantioselectivity (85% yield and 94% ee).

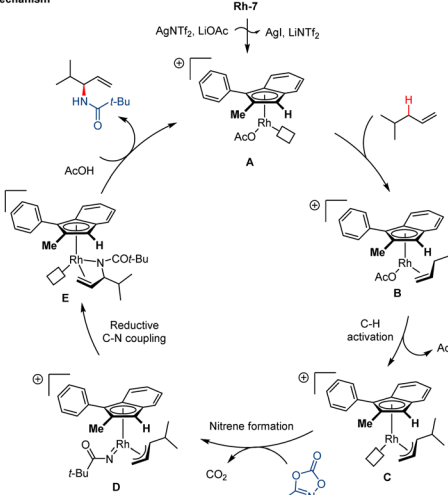
Recently, Wang and coworkers reported a chiral  $\text{Cp}^x\text{Rh}(\text{III})$ -catalyzed asymmetric allylic C–H amination of unactivated terminal alkenes using sulfonamides as readily accessible nitrogen sources (Scheme 15).<sup>71</sup> Employing  $\text{Cp}^x\text{Rh}(\text{III})$  catalyst **Rh-6**, this transformation establishes a robust platform for synthesizing chiral allylic amines in excellent yields (up to 99%) with exceptional regioselectivity (>20:1 B/L) and high enantioselectivity (up to 96% ee). In this system, sulfonamides are converted *in situ* by  $\text{PhI}(\text{OPiv})_2$  into reactive iminoiodinane species,



## Selected examples:



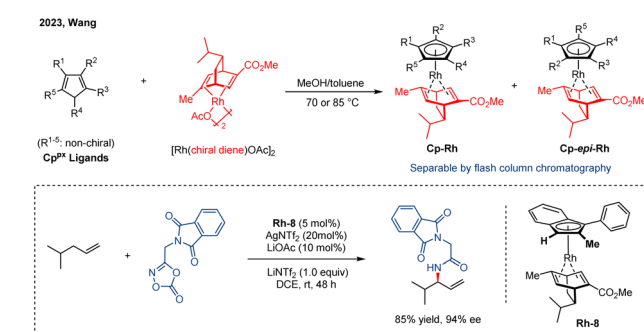
## Proposed mechanism



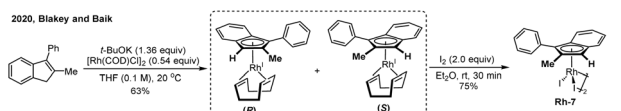
Scheme 13 Rh(III)-catalyzed asymmetric allylic C( $\text{sp}^3$ )-H amidation of unactivated olefins.

which serve as the key nitrene precursors. The reaction scope extends to internal alkenes, as demonstrated with *(E)*-4-octene, which afforded two regioisomers in a 1:3 ratio with moderate enantioselectivity. A proposed mechanism begins with allylic C–H activation to form a metal–allyl intermediate **II**. This intermediate is intercepted by the *in situ*-generated iminoiodinane, yielding the allyl–Rh–nitrenoid species **IV**. Subsequent C–N reductive coupling forms complex **V**, and final protodemetalation releases the chiral amide product. Mechanistic studies indicate that the allylic C–H bond cleavage is irreversible and the rate-determining step, and is also critical for enantiocontrol.

Very recently, Shi and coworkers developed a novel class of planar chiral AtroInd–rhodium(III) complexes (atropisomeric

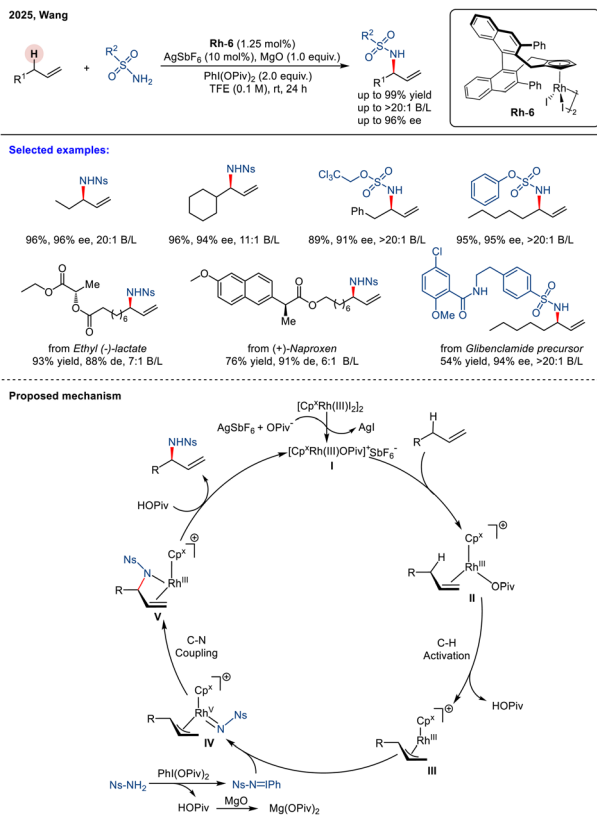


Scheme 14 Synthesis and evaluation of planar chiral  $\text{Cp}^x\text{Rh}$  complexes.



Scheme 12 Synthesis of planar chiral indenyl–rhodium complexes.

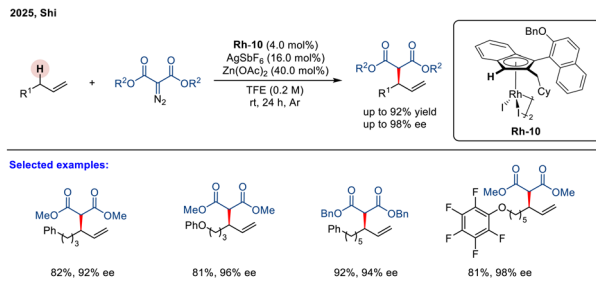




Scheme 15 Rh(III)-catalyzed enantioselective intermolecular allylic C–H amination of unactivated alkenes.

indenyl-derived rhodium(III) complexes) that enabled the asymmetric allylic C–H amination of unactivated terminal alkenes using sulfonamides as readily available nitrogen sources (Scheme 16).<sup>72</sup> This transformation represents a significant advance in the field of allylic C–H amination. With the  $\text{Cp}^x\text{Rh(III)}$  catalyst **Rh-10**, the reaction proceeds smoothly at 65 °C to furnish a wide range of enantioenriched allylic amines in excellent yields (up to 98%) and outstanding enantioselectivities (up to 99% ee).

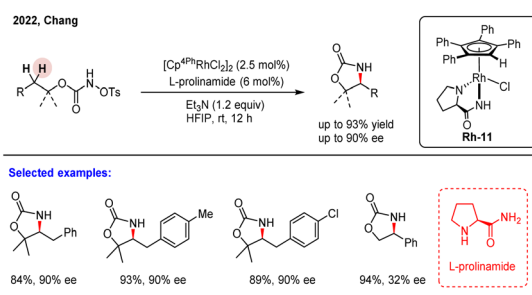
In general,  $\text{Cp}^x\text{M(III)}$ -catalyzed amidation reactions *via* the nitrene transfer pathway follow an inner-sphere or outer-sphere mechanism.<sup>34</sup> While inner-sphere amidation forms a metacyclic intermediate with the assistance of a directing group, the outer-sphere mechanism involves an external ligand engaged C–H insertion or stepwise hydrogen atom transfer (HAT) and C–N bond formation process, thereby providing an opportunity to induce enantioselectivity. In 2022, Chang and co-workers developed a multidimensional screening platform for the rapid *in situ* generation of half-sandwich metal complexes, enabling simultaneous evaluation of metal centers,  $\text{Cp}^x\text{Rh}$  precatalysts, co-ligands, and nitrene precursors.<sup>56</sup> This approach facilitated the efficient identification of optimal  $\text{Cp}^x\text{Rh(III)}$ -co-ligand catalysts for both intra- and intermolecular C–H amidation reactions. Moreover, the high-throughput strategy was successfully extended to the development of a chiral catalytic system for enantioselective intramolecular amidation using *N*-tosyloxycarbamates as nitrene precursors.



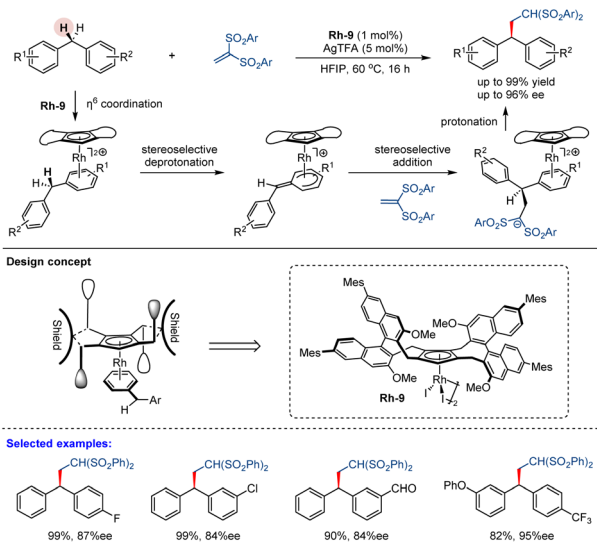
Scheme 16 Rh(III)-catalyzed asymmetric intermolecular allylic C–H amination of unactivated alkenes.

The optimal catalytic system for asymmetric intramolecular C–H amidation was identified as the *in situ* generated complex **Rh-11**, comprising an achiral  $\text{Cp}^{4\text{Ph}}$  ligand and a chiral L-prolinamide co-ligand. This system afforded chiral 2-oxazolidinones (four examples) in good yields with high enantioselectivities (up to 90% ee, Scheme 17). Although excellent stereocontrol was achieved, the substrate scope evaluation revealed that high enantioselectivity is strongly dependent on the structure of the substituents and particularly sensitive to structural variations. This limitation highlights the need for the development of more versatile and efficient chiral rhodium catalysts for this class of asymmetric C–H amidation.

In a general asymmetric induction model, chiral Cp ligands could provide a semi-enclosed environment through the chiral backbone (back wall) and substituents on the Cp ligand (side wall). However, these chiral Cp ligands were less efficient for  $\pi$ -coordination-enabled benzylic C–H bond functionalization, because ligated arene and/or the C(aryl)–C(benzylic) bond can rotate, and the benzylic position is distal to these ligands. In 2024, Shi, You and co-workers developed a novel class of chiral Cp ligands featuring two identically substituted binaphthyl groups.<sup>73</sup> By using **Rh-9** as the catalyst, they achieved the asymmetric C–H bond activation of diarylmethanes bearing *meta*- and/or *para*-differentiated aryl motifs to 1,1-bis(arylsulfonyl)ethylenes in high yields (up to 99%) and excellent enantioselectivity (up to 96% ee) (Scheme 18). The authors anticipated that coordination of one arene ring of the diarylmethane to the **Rh-9** center forms a rigid complex, where the sterically confined pocket constructed by the Cp ring and two nonparallel naphthyl walls restricts rotation of the bound arene ring. This spatial constraint facilitates stereoselective



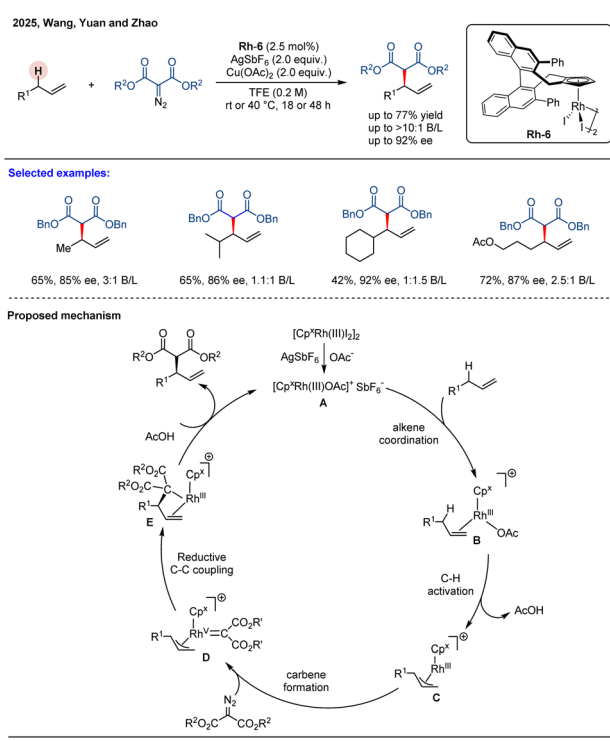
Scheme 17 Piano-stool type Rh(III)-catalyzed enantioselective intramolecular C–H amidation.



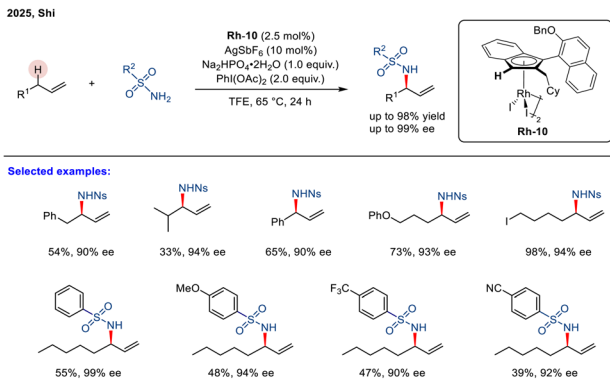
**Scheme 18** Rh(III)-catalyzed desymmetrization of diarylmethanes.

functionalization of the benzylic C-H bonds *via* a sequential arene-selective  $\eta^6$  coordination, stereoselective deprotonation, and stereoselective addition process, ultimately affording chiral diarylmethanes.

In 2025, Wang, Yuan, and co-workers developed an asymmetric allylic C–H alkylation of unactivated alkenes with  $\alpha$ -di-azocarbonyl compounds using a BINOL-derived chiral cyclopentadienyl rhodium catalyst **Rh-6** (Scheme 19).<sup>74</sup> This method provides efficient access to chiral products with good



**Scheme 19** Rh(III)-catalyzed asymmetric allylic C–H alkylation of unactivated alkenes



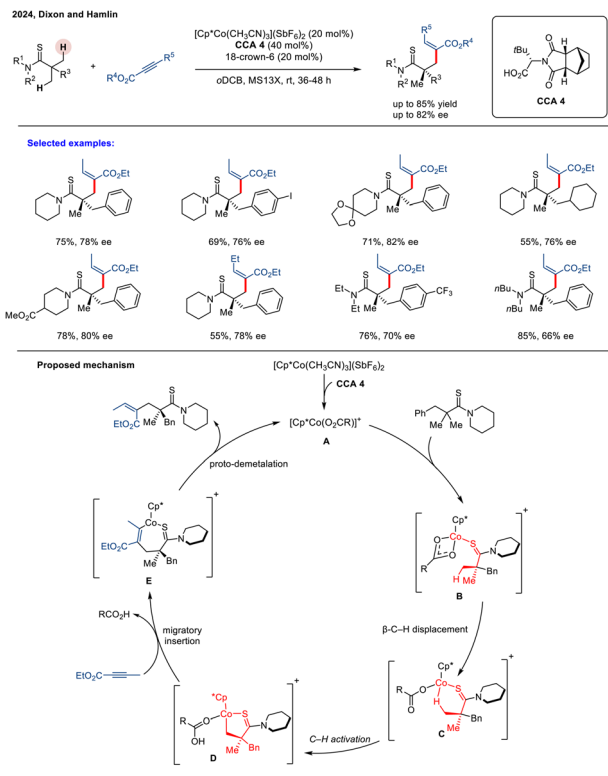
**Scheme 20** Rh(III)-catalyzed asymmetric allylic C–H alkylation of  $\alpha$ -olefins

yields (up to 77%), high enantioselectivity (up to 92% ee), and regiocontrol (>10:1 B/L ratio). The reaction demonstrates broad substrate scope, accommodating both aliphatic and aryl-substituted terminal alkenes. Competitive and parallel KIE experiments indicate that the allylic C–H bond cleavage is the rate-determining step in the catalytic cycle. The reaction is initiated by the formation of a cationic  $\text{Cp}^*\text{Rh}$  complex **A**, which is generated through activation of the dimeric precatalyst by  $\text{AgSbF}_6$  and  $\text{Cu}(\text{OAc})_2$ . Subsequently, coordination of the alkene to complex **A** gives intermediate **B**, which then undergoes a rate- and enantio-determining allylic C–H activation to afford the  $\pi$ -allyl Rh(III) species **C**. Following this, reaction with the diazo compound leads to the formation of a Rh(V)–carbene intermediate **D**. Next, reductive elimination from **D** furnishes complex **E**, which finally undergoes protonolysis to release the chiral product and regenerate the catalytically active Rh(III) species. Although this work constitutes an advance in asymmetric allylic C–H functionalization, the modest enantioselectivity and B/L selectivity for some substrates highlight areas for further optimization to broaden its applicability.

Very recently, Shi and coworkers disclosed a related strategy for the asymmetric allylic C–H alkylation of terminal olefins, utilizing diazo compounds as convenient alkylating agents (Scheme 20).<sup>75</sup> The deployment of a newly designed chiral AtroInd–rhodium(III) catalyst system enabled remarkable command over chemoselectivity, regioselectivity, and enantioselectivity. This catalytic system proved broadly applicable, delivering a wide scope of enantioenriched products in excellent yields (up to 92%) and with high enantiomeric excess (up to 98% ee). Mechanistically, competitive and parallel kinetic isotope effect (KIE) studies identified allylic C–H bond cleavage as the rate-determining event.

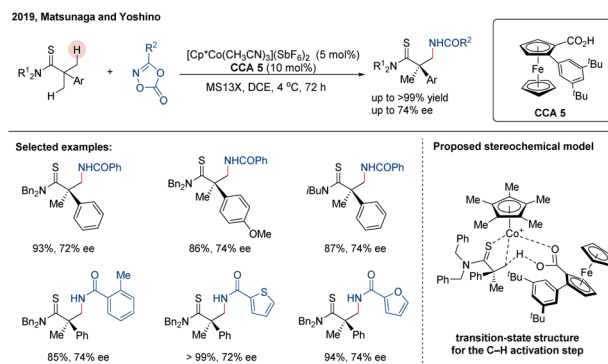
### 3 $\text{Cp}^x\text{Co}(\text{III})$ -catalyzed asymmetric $\text{C}(\text{sp}^3)-\text{H}$ functionalization

High-valent Cp<sup>\*</sup>Co(III) complexes have garnered significant attention due to their earth abundance, low cost, and notable reactivity in C–H functionalization. In 2017, Dixon, Seayad and co-workers reported a Cp<sup>\*</sup>Co(III)-catalyzed C(sp<sup>3</sup>)–H amidation of



Scheme 21 Co(III)/CCA-catalyzed enantioselective  $C(sp^3)$ -H amidation of thioamides.

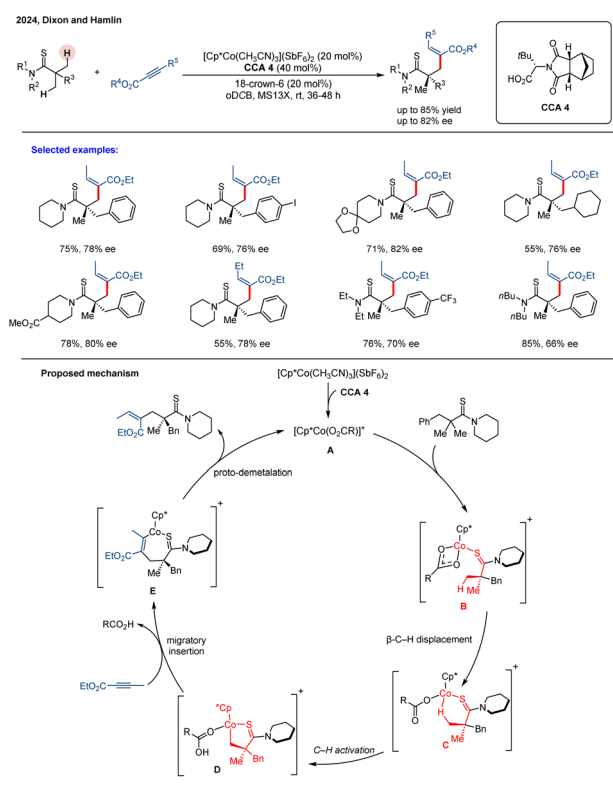
thioamides using dioxazolones as amidating agents.<sup>76</sup> Computational studies revealed that the key cyclometalation step proceeds *via* an external carboxylate-assisted concerted metalation-deprotonation (CMD) mechanism, shedding light on the mechanistic features governing reactivity and selectivity in this transformation. Inspired by the seminal work of Dixon and Seayad, Matsunaga and co-workers reported an achiral  $Cp^*Co(III)$ /chiral carboxylic acid hybrid catalytic system for the asymmetric  $C(sp^3)$ -H amidation of thioamides, employing a desymmetrization strategy.<sup>77</sup> In this study, the authors evaluated several readily available amino acid-derived chiral carboxylic acids (CCAs) as ligands. The *tert*-leucine-derived CCA 5 was identified as optimal. Furthermore, modification of the cobalt catalyst revealed that the



Scheme 22 Co(III)-ferrocene carboxylic acid catalyzed enantioselective  $C(sp^3)$ -H amidation of  $\alpha$ -aryl thioamides.

more sterically hindered  $Cp^*\ell BuCo(III)$  complex provided the highest enantioselectivity, albeit with a slight reduction in reactivity. A series of chiral  $\beta$ -amino thiocarbonyl building blocks containing quaternary stereocenters were successfully synthesized, achieving moderate to good enantioselectivities of up to 88% ee (Scheme 21). Mechanistically, the active species  $Cp^*Co(O_2CR)^+$  may form between  $Cp^*Co(III)$  and the chiral acid co-catalyst CCA 4, possibly aided by the basic substrates. Subsequent binding of the thioamide substrate generates intermediate B, which undergoes cyclometallation *via* a carboxylate-assisted concerted metalation-deprotonation (CMD) process to yield the cobaltacycle intermediate D. This C-H activation step was shown to be both irreversible and the enantioselectivity-determining step. Coordination of the dioxazolone followed by migratory insertion of the nitrenoid moiety furnishes intermediate F. Finally, protonolysis of the cobalt–carbon bond in F releases the chiral product and regenerates the active catalytic species, thereby completing the catalytic cycle.

In 2019, Matsunaga group developed new planar chiral ferrocene-based carboxylic acids as chiral co-ligands for this  $Cp^*Co(III)$ -catalyzed enantioselective C-H amidation of thioamides (Scheme 22).<sup>78</sup> These chiral 2-aryl ferrocene carboxylic acids (CCAs) were synthesized *via* a highly efficient diastereoselective *ortho*-lithiation/Suzuki–Miyaura cross-coupling sequence, enabling a modular and versatile ligand scaffold. Systematic screening identified the sterically encumbered ligand CCA 5 as optimal, although the system provided only moderate enantioselectivity (up to 74% ee) despite high



Scheme 23 Co(III)/CCA-catalyzed enantio- and regioselective  $C(sp^3)$ -H alkenylation of thioamides.



reactivity. The authors proposed a stereochemical model wherein enantioinduction arises from minimizing steric repulsion between the substrate and the chiral ligand environment.

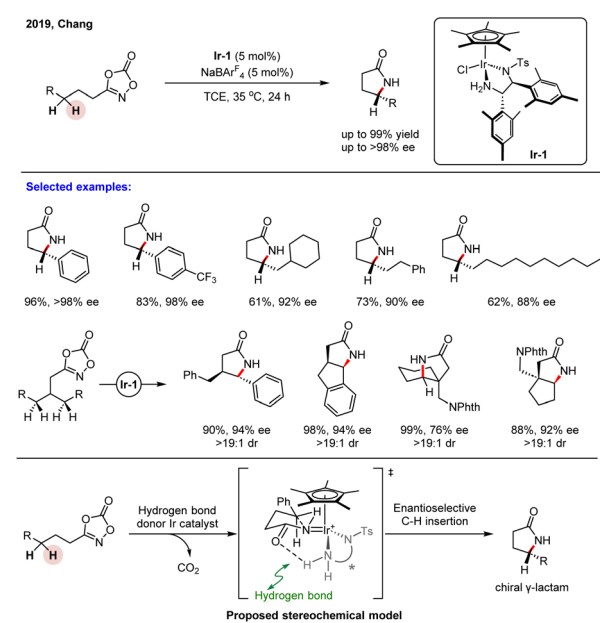
In 2024, Dixon and co-workers developed a  $\text{Cp}^*\text{Co}(\text{m})$ -catalyzed asymmetric  $\text{C}(\text{sp}^3)\text{-H}$  alkenylation of thioamides using but-2-ynoate esters as coupling partners.<sup>79</sup> The reaction utilized an achiral  $\text{Cp}^*\text{Co}$  complex with a chiral carboxylic acid as the catalyst. Screening of various amino acid-derived CCAs identified *tert*-leucine-derived **CCA 3** as optimal, providing the highest enantioselectivity. While the direct reaction gave moderate enantiomeric excess (up to 82% ee), recrystallization afforded enantiopure products (>99:1 er). These enantioenriched compounds were further diversified into various valuable, complex scaffolds, demonstrating the method's synthetic utility. Complementary computational studies revealed that steric repulsions govern both enantioselectivity in the  $\text{C-H}$  activation step and regioselectivity during migratory insertion (Scheme 23). The catalytic cycle begins with thioamide coordination to form complex **B**.  $\text{C-H}$  activation then proceeds *via* a  $\kappa^2$ -to- $\kappa^1$  carboxylate displacement by the substrate's  $\beta$ -hydrogen (**C**), following a CMD mechanism to generate cobaltacycle **D**. A steric clash between the chiral co-catalyst's *t*Bu group and the substrate's benzyl group plays a critical role in establishing stereocontrol in this step. Subsequent alkyne migratory insertion affords intermediate **E**, and protonolysis releases the product while regenerating the active  $\text{Cp}^*\text{Co}(\text{O}_2\text{-CR})^+$  catalyst. Despite these advances, the requirement for a high catalyst loading (20 mol%) could hinder practical scalability. This limitation highlights the necessity for developing more active and robust chiral  $\text{Cp}^*\text{Co}(\text{m})$  catalytic systems capable of operating at lower loadings while providing enhanced asymmetric induction.

## 4 $\text{Cp}^*\text{Ir}(\text{III})$ -catalyzed asymmetric $\text{C}(\text{sp}^3)\text{-H}$ functionalization

Cyclometallated  $\text{Cp}^*\text{Ir}(\text{III})$  complexes are well-established for promoting  $\text{C-H}$  activation *via* inner-sphere mechanisms; however, enantioselective  $\text{C}(\text{sp}^3)\text{-H}$  functionalization using such pathways remains challenging. In a 2018 breakthrough, Chang and co-workers demonstrated that  $\text{Cp}^*\text{Ir}(\text{III})$  complexes, when leveraged with electron-donating bidentate ligands, could achieve intramolecular  $\text{C}(\text{sp}^3)\text{-H}$  amidation through an outer-sphere mechanism, enabling the highly selective synthesis of  $\gamma$ -lactams from 1,4,2-dioxazol-5-ones.<sup>80</sup> Building on this, they subsequently developed a  $\text{Cp}^*\text{Ir}(\text{III})$ -catalyzed asymmetric intramolecular  $\text{C}(\text{sp}^3)\text{-H}$  amidation for synthesizing chiral  $\gamma$ -lactams—privileged scaffolds prevalent in natural products and bioactive compounds (Scheme 24).<sup>54</sup> Through systematic evaluation of  $N,O$ - and  $N,N'$ -bidentate chiral ligands, an  $N,N'$ -donor ligand (**Ir-1**) was identified as optimal. The reaction exhibited a broad substrate scope, efficiently converting readily accessible dioxazolones into  $\gamma$ -lactams in high yield with excellent enantioselectivity. It proved compatible with diverse secondary  $\text{C-H}$  bonds—including benzylic, unactivated aliphatic,

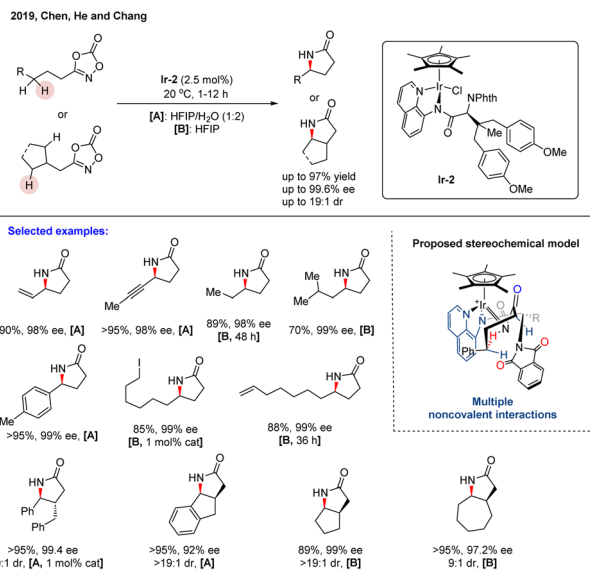
propargylic, and allylic sites—delivering products with high regio- and stereocontrol. Mechanistic studies, supported by DFT calculations, indicated that hydrogen-bonding interactions between the substrate and chiral catalyst are pivotal in the enantio-determining step. Notably, the methodology was successfully applied to the desymmetrization of meso-substrates, enabling the simultaneous installation of two contiguous stereocenters in a single transformation. This work underscores the potential of outer-sphere  $\text{Ir}(\text{III})$  catalysis for asymmetric  $\text{C}(\text{sp}^3)\text{-H}$  functionalization and opens up new avenues for the precise construction of complex chiral architectures.

In the same year, Chen, He, Chang, and co-workers reported a highly enantioselective intramolecular  $\text{C}(\text{sp}^3)\text{-H}$  amidation catalyzed by a newly designed,  $\alpha$ -amino-acid-based ligand in combination with  $\text{Cp}^*\text{Ir}(\text{III})$ .<sup>55</sup> Through systematic ligand exploration, they identified the pre-formed, diarylated complex **Ir-2**—derived from an aminoquinoline (AQ)-appended chiral amide—as the optimal catalyst, which provided both high reactivity and excellent enantioselectivity (Scheme 25). This system efficiently converted dioxazolones into optically enriched  $\gamma$ -lactams, demonstrating broad functional group tolerance across diverse secondary  $\text{C-H}$  bonds (including benzylic, unactivated aliphatic, propargylic, and allylic sites) and proving effective in desymmetrization reactions. Mechanistic studies revealed that the  $\text{Cp}^*$ , AQ, and phthalimide (Phth) groups in **Ir-2** collectively generate an enzyme-like hydrophobic pocket around the iridium center. This distinctive architecture promotes efficient substrate binding and conversion, even in polar or aqueous media. Notably, enantiocontrol is achieved *via* a network of noncovalent interactions—primarily  $\pi$ - $\pi$  stacking and hydrogen bonding—rather than through traditional steric repulsion. This work establishes a distinct biomimetic



Scheme 24 Piano-stool type  $\text{Ir}(\text{III})$ -catalyzed asymmetric intramolecular  $\text{C}(\text{sp}^3)\text{-H}$  amidation of dioxazolone.





**Scheme 25** Piano-stool type Ir(III)-catalyzed enantioselective intramolecular C(sp<sup>3</sup>)-H amidation of dioxazolone.

paradigm for enantioinduction and expands the toolbox for designing sophisticated chiral transition metal catalysts.

Artificial metalloenzymes (ArMs) represent a powerful class of hybrid catalysts that combine synthetic metal centers with protein scaffolds.<sup>81-83</sup> This strategy merges the versatile reactivity of organometallic catalysis with the exquisite selectivity and evolvability of biological systems. To unlock their full potential, a synergistic approach is essential, involving precise chemical modification of the metal cofactor alongside protein engineering of the host to control catalytic activity and stereoselectivity.

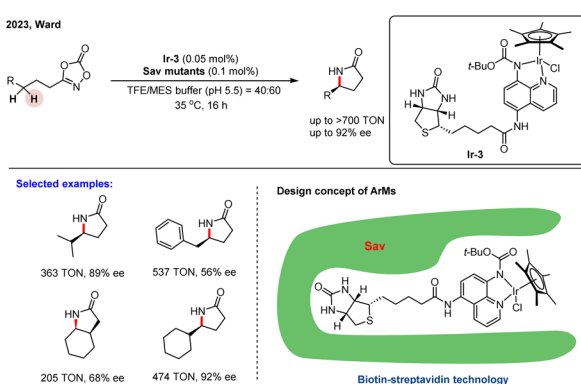
A significant advance in this field was reported by Ward and co-workers, who constructed an artificial metalloenzyme for the enantioselective amidation of unactivated C(sp<sup>3</sup>)-H bonds using biotin-streptavidin (Sav) technology.<sup>84</sup> They incorporated a series of biotinylated Cp<sup>x</sup>Ir(III) cofactors into the Sav scaffold to generate chiral catalytic ArMs. These assemblies promoted intramolecular C-H amidation to form  $\gamma$ -lactams with high regioselectivity and moderate enantioselectivity. The cofactor

[Cp<sup>x</sup>Ir(Boc-AQ-biot)Cl] (**Ir-3**) showed the best initial performance, affording the product with 47 turnovers (TON) and 30% ee. To improve stereocontrol, the authors employed iterative saturation mutagenesis to evolve the protein's secondary coordination sphere. This engineering strategy yielded a significantly improved variant capable of achieving up to 308 TON and 86% ee. Subsequent substrate scope evaluation demonstrated that the optimized ArM could reach enantiomeric excesses of up to 92%, highlighting its potential as a useful platform for asymmetric C-H functionalization (Scheme 26).

## 5 The challenge of asymmetric C(sp<sup>3</sup>)-H functionalization with Cp<sup>x</sup>M(III) (M = Co, Rh, Ir) catalysts

Although asymmetric C(sp<sup>3</sup>)-H functionalization catalyzed by Cp<sup>x</sup>M(III) complexes (M = Co, Rh, Ir) has emerged as a transformative strategy in modern organic synthesis, several critical challenges continue to impede its broader application. Chief among these is the fundamental inertness of C(sp<sup>3</sup>)-H bonds, which exhibit low acidity, lack polarity, and often reside in sterically congested environments. These intrinsic properties demand the development of highly efficient, site-selective, and stereochemically defined catalytic systems capable of overcoming formidable kinetic and thermodynamic barriers.

Attaining high levels of enantioselectivity remains particularly demanding. It necessitates precise control over the chiral environment at the metal center, which must be delicately tuned through rational ligand design and chiral catalyst development. The development of chiral Cp<sup>x</sup> ligands that are both broadly applicable and capable of differentiating between similar C-H bonds in complex settings is still in its infancy. The reported chiral catalysts have primarily considered different types of chiral backbones to introduce a suitable chiral environment and achieve a high level of asymmetric control. However, the chiral environment directly on the metal center—closest to the reactive site—has received less attention as a tool for tuning catalytic activity and asymmetric induction. This underexplored area presents a significant opportunity for more diverse catalyst design. In addition, the reported synthesis of chiral Cp<sup>x</sup> ligands and their corresponding metal complexes often involves multiple steps. This significantly increases their cost, hinders large-scale preparation, and limits their widespread application. Furthermore, the catalytic potential and intrinsic reactivity differences among Rh-, Ir-, and Co-based Cp<sup>x</sup> M(III) systems have not yet been systematically explored or directly compared, which presents a significant opportunity for further development. Beyond the commonly studied M(III) oxidation state, catalysts based on alternative metal oxidation states (like the M(I) oxidation state) also remain largely unexplored. These systems may offer distinct reactivity patterns and unique mechanistic pathways for asymmetric C(sp<sup>3</sup>)-H functionalization. Consequently, the development of more streamlined, modular, and scalable synthetic routes to chiral catalysts with diverse electronic and steric properties remains a critical and highly desirable objective in the field.



**Scheme 26** ArM catalyzed asymmetric intramolecular C(sp<sup>3</sup>)-H amidation of dioxazolone.

The substrate scope for asymmetric  $\text{Cp}^x\text{M}(\text{iii})$ -catalyzed  $\text{C}(\text{sp}^3)\text{-H}$  functionalization is often limited by sensitivity to polar or coordinating functional groups. Furthermore, the regio- and enantioselective activation of challenging unactivated  $\text{C}(\text{sp}^3)\text{-H}$  bonds (*e.g.*, in alkanes) remains a major unsolved challenge. Furthermore, despite substantial methodological progress, the application of this strategy to the synthesis of complex natural products and pharmaceuticals remains underdeveloped. Most studies rely on simplified model substrates, while examples of late-stage functionalization of architecturally complex bioactive molecules are rare. Continued efforts in this direction will be important for fully realizing the synthetic potential of this strategy in medicinal chemistry and natural product synthesis. Overcoming these hurdles would greatly enhance the method's synthetic power.

Key mechanistic aspects—including the nature of metal–carbon bond formation, the role of concerted-metallation–deprotonation (CMD) *versus* outer-sphere pathways, and the origin of stereoselectivity—require further elucidation to guide rational catalyst design and enable novel, challenging transformations. In particular, a systematic, predictive understanding of how the steric and electronic parameters of  $\text{Cp}^x\text{M}(\text{iii})$  complexes influence catalytic performance is lacking. Dedicated studies aimed at establishing structure–activity relationships through integrated experimental and computational (DFT) approaches are needed to unlock the potential of this catalytic system in asymmetric  $\text{C}(\text{sp}^3)\text{-H}$  functionalization.

Addressing these challenges will require a synergistic integration of ligand innovation, mechanistic insight, and synthetic methodology development. Emerging tools such as high-throughput experimentation, *in situ* spectroscopic techniques, and computational modelling hold promise for accelerating catalyst discovery and reaction optimization. Expanding the scope of compatible substrates, enhancing catalyst robustness, and simplifying operational protocols are essential next steps in establishing asymmetric  $\text{C}(\text{sp}^3)\text{-H}$  functionalization as a general and practical platform for stereoselective synthesis.

## 6 Summary and outlook

Enantioselective  $\text{C}(\text{sp}^3)\text{-H}$  functionalization mediated by group 9  $\text{Cp}^x\text{M}(\text{iii})$  complexes ( $\text{M} = \text{Co, Rh, Ir}$ ) has emerged as a transformative paradigm for the direct catalytic assembly of stereogenic centers. This review comprehensively examines strategic advances in catalyst design—encompassing tailored chiral cyclopentadienyl ( $\text{Cp}^x$ ) ligands, cooperative chiral carboxylic acid (CCA) auxiliaries, and modular bidentate coordination complexes—that have enabled remarkable regio- and enantiocontrol in the functionalization of challenging  $\text{sp}^3$ -hybridized C–H bonds.

While substantial progress has been made, the field continues to face fundamental challenges, including limited reaction types, narrow substrate scope, and modest catalyst efficiency. Overcoming these limitations will require deepened mechanistic insight and innovative ligand architectures, particularly for earth-abundant cobalt catalysts. The broad synthetic utility of these methods—spanning complex molecule

synthesis, pharmaceutical development, and materials science—underscores their potential to redefine retrosynthetic planning.

$\text{Cp}^x\text{M}(\text{iii})$ -catalyzed asymmetric  $\text{C}(\text{sp}^3)\text{-H}$  functionalization is a rapidly advancing frontier in organic synthesis. This review critically analyses the field's current achievements and identifies persistent challenges to map a path toward more practical, efficient, and sustainable stereoselective strategies. Ultimately, we aim to provide not only a comprehensive overview but also to inspire further exploration, accelerating the development of scalable methods for the synthesis of complex chiral molecules.

## Author contributions

Shu-Bin Mou: writing-original draft, methodology. Mu-Peng Luo: writing-review & editing, Feifei Fang: writing-review & editing. Shi Cao: writing-review & editing, supervision. Dong Wu: review, supervision, project administration. Shou-Guo Wang: supervision, project administration, funding acquisition.

## Conflicts of interest

The authors declare no conflict of interest.

## Data availability

No primary research results, software or code have been included and no new data were generated or analysed as part of this review.

## Acknowledgements

This work was supported by Guangdong Basic and Applied Basic Research Foundation (2024A1515011368 and 2024QN11C213); the Scientific Foundation for Youth Scholars of Shenzhen University (868-000001033009); and the National Natural Science Foundation of China (22333006). S.-G. is indebted to Shenzhen University for providing a start-up grant.

## References

- 1 A. García-Viada, J. C. Carretero, J. Adrio and N. Rodríguez, *Chem. Soc. Rev.*, 2025, **54**, 4353–4390.
- 2 J. Grover, A. T. Sebastian, S. Maiti, A. C. Bissember and D. Maiti, *Chem. Soc. Rev.*, 2025, **54**, 2006–2053.
- 3 J. F. Hartwig, *J. Am. Chem. Soc.*, 2016, **138**, 2–24.
- 4 I. F. Yu, J. W. Wilson and J. F. Hartwig, *Chem. Rev.*, 2023, **123**, 11619–11663.
- 5 B. Liu, A. M. Romine, C. Z. Rubel, K. M. Engle and B. F. Shi, *Chem. Rev.*, 2021, **121**, 14957–15074.
- 6 S. K. Sinha, S. Guin, S. Maiti, J. P. Biswas, S. Porey and D. Maiti, *Chem. Rev.*, 2022, **122**, 5682–5841.
- 7 O. Baudoin, *Chem. Soc. Rev.*, 2011, **40**, 4902–4911.
- 8 R. Bisht, C. Halder, M. M. M. Hassan, M. E. Hoque, J. Chaturvedi and B. Chattopadhyay, *Chem. Soc. Rev.*, 2022, **51**, 5042–5100.



9 L. Ping, D. S. Chung, J. Bouffard and S.-G. Lee, *Chem. Soc. Rev.*, 2017, **46**, 4299–4328.

10 H. Huang, X. Ji, W. Wu and H. Jiang, *Chem. Soc. Rev.*, 2015, **44**, 1155–1171.

11 J. A. Labinger and J. E. Bercaw, *Nature*, 2002, **417**, 507–514.

12 J. H. Docherty, T. M. Lister, G. McArthur, M. T. Findlay, P. Domingo-Legarda, J. Kenyon, S. Choudhary and I. Larrosa, *Chem. Rev.*, 2023, **123**, 7692–7760.

13 B. M. Trost, *Science*, 1991, **254**, 1471–1477.

14 C. G. Newton, S. G. Wang, C. C. Oliveira and N. Cramer, *Chem. Rev.*, 2017, **117**, 8908–8976.

15 R. Giri, B. F. Shi, K. M. Engle, N. Maugel and J. Q. Yu, *Chem. Soc. Rev.*, 2009, **38**, 3242–3272.

16 H.-H. Li, X. Chen and S. Kramer, *Chem. Sci.*, 2023, **14**, 13278–13289.

17 X. Yu, Z.-Z. Zhang, J.-L. Niu and B. F. Shi, *Org. Chem. Front.*, 2022, **9**, 1458–1484.

18 Q. Zhang, L.-S. Wu and B.-F. Shi, *Chem.*, 2022, **8**, 384–413.

19 T. G. Saint-Denis, R.-Y. Zhu, G. Chen, Q.-F. Wu and J.-Q. Yu, *Science*, 2018, **359**, eaao4798.

20 J. Pedroni and N. Cramer, *Chem. Commun.*, 2015, **51**, 17647–17657.

21 J. He, M. Wasa, K. S. L. Chan, Q. Shao and J. Q. Yu, *Chem. Rev.*, 2017, **117**, 8754–8786.

22 P. S. Wang and L. Z. Gong, *Acc. Chem. Res.*, 2020, **53**, 2841–2854.

23 K. Yang, M. Song, H. Liu and H. Ge, *Chem. Sci.*, 2020, **11**, 12616–12632.

24 C.-X. Liu, S.-Y. Yin, F. Zhao, H. Yang, Z. Feng, Q. Gu and S.-L. You, *Chem. Rev.*, 2023, **123**, 10079–10134.

25 B. Ye and N. Cramer, *Acc. Chem. Res.*, 2015, **48**, 1308–1318.

26 G. Song, F. Wang and X. Li, *Chem. Soc. Rev.*, 2012, **41**, 3651–3678.

27 Y. Zhang, J.-J. Zhang, L. Lou, L. Lin, N. Cramer, S.-G. Wang and Z. Chen, *Chem. Soc. Rev.*, 2024, **53**, 3457–3484.

28 K. Yamakawa and T. Nishimura, *Chem. Commun.*, 2025, **61**, 13094–13108.

29 R. Kaur and N. Jain, *Chem. Asian J.*, 2022, **17**, e202200944.

30 T. Nishimura, *Chem. Rec.*, 2021, **21**, 3532–3545.

31 Ł. Woźniak, J.-F. Tan, Q.-H. Nguyen, A. M. Vigné, V. Smal, Y.-X. Cao and N. Cramer, *Chem. Rev.*, 2020, **120**, 10516–10543.

32 B. Garai, A. Das, D. V. Kumar and B. Sundararaju, *Chem. Commun.*, 2024, **60**, 3354–3369.

33 Q. J. Yao and B. F. Shi, *Acc. Chem. Res.*, 2025, **58**, 9719–9990.

34 J. Lee and S. Chang, *Synlett*, 2023, **34**, 1356–1366.

35 Y. Zheng, C. Zheng, Q. Gu and S. L. You, *Chem. Catal.*, 2022, **2**, 2965–2985.

36 P. Gandeepan, T. Müller, D. Zell, G. Cera, S. Warratz and L. Ackermann, *Chem. Rev.*, 2019, **119**, 2192–2452.

37 J. Mo, A. M. Messinis, J. Li, S. Warratz and L. Ackermann, *Acc. Chem. Res.*, 2024, **57**, 10–22.

38 Ł. Woźniak and N. Cramer, *Trends Chem.*, 2019, **1**, 471–484.

39 J. Loup, U. Dhawa, F. Pesciaioli, J. Wencel-Delord and L. Ackermann, *Angew. Chem., Int. Ed.*, 2019, **58**, 12803–12818.

40 X.-J. Si, T.-C. Wang, T.-P. Loh and M.-Z. Lu, *Chem. Sci.*, 2025, **16**, 5836–5848.

41 Y. He, Z. Huang, K. Wu, J. Ma, Y.-G. Zhou and Z. Yu, *Chem. Soc. Rev.*, 2022, **51**, 2759–2852.

42 T. K. Achar, S. Maiti, S. Jana and D. Maiti, *ACS Catal.*, 2020, **10**, 13748–13793.

43 T. K. Hyster, L. Knörr, T. R. Ward and T. Rovis, *Science*, 2012, **338**, 500–503.

44 B. Ye and N. Cramer, *Science*, 2012, **338**, 504–506.

45 C. Davies, S. Shaaban and H. Waldmann, *Trends Chem.*, 2022, **4**, 318–330.

46 J. Mas-Roselló, A. G. Herraiz, B. Audic, A. Laverny and N. Cramer, *Angew. Chem., Int. Ed.*, 2021, **60**, 13198–13224.

47 S. Shaaban, C. Davies and H. Waldmann, *Eur. J. Org. Chem.*, 2020, 6512–6524.

48 T. Yoshino, S. Satake and S. Matsunaga, *Chem.–Eur. J.*, 2020, **26**, 7346–7357.

49 T. Yoshino and S. Matsunaga, *ACS Catal.*, 2021, **11**, 6455–6466.

50 C. Pan, S. Y. Yin, Q. Gu and S. L. You, *Org. Biomol. Chem.*, 2021, **19**, 7264–7275.

51 P.-F. Qian, J.-Y. Li, Y.-B. Zhou, T. Zhou and B.-F. Shi, *SynOpen*, 2023, **07**, 466–485.

52 S. K. Sinha, P. Ghosh, S. Jain, S. Maiti, S. A. Al-Thabati, A. A. Alshehri, M. Mokhtar and D. Maiti, *Chem. Soc. Rev.*, 2023, **52**, 7461–7503.

53 C. G. Newton, D. Kossler and N. Cramer, *J. Am. Chem. Soc.*, 2016, **138**, 3935–3941.

54 Y. Park and S. Chang, *Nat. Catal.*, 2019, **2**, 219–227.

55 H. Wang, Y. Park, Z. Bai, S. Chang, G. He and G. Chen, *J. Am. Chem. Soc.*, 2019, **141**, 7194–7201.

56 J. Jeong, H. Jung, D. Kim and S. Chang, *ACS Catal.*, 2022, **12**, 8127–8138.

57 H. Li, R. Gontla, J. Flegel, C. Merten, S. Ziegler, A. P. Antonchick and H. Waldmann, *Angew. Chem., Int. Ed.*, 2019, **58**, 307–311.

58 C. Ma, P. Fang and T.-S. Mei, *ACS Catal.*, 2018, **8**, 7179–7189.

59 Y.-Q. Huang, Z.-J. Wu, L. Zhu, Q. Gu, X. Lu, S.-L. You and T.-S. Mei, *CCS Chem.*, 2022, **4**, 3181–3189.

60 W. Wei, A. Scheremetjew and L. Ackermann, *Chem. Sci.*, 2022, **13**, 2783–2788.

61 S. Fukagawa, M. Kojima, T. Yoshino and S. Matsunaga, *Angew. Chem., Int. Ed.*, 2019, **58**, 18154–18158.

62 L.-T. Huang, S. Fukagawa, M. Kojima, T. Yoshino and S. Matsunaga, *Org. Lett.*, 2020, **22**, 8256–8260.

63 Z.-Y. Zhang, B.-B. Gou, Q. Wang, Q. Gu and S.-L. You, *Adv. Synth. Catal.*, 2024, **366**, 774–779.

64 Y. Kato, L. Lin, M. Kojima, T. Yoshino and S. Matsunaga, *ACS Catal.*, 2021, **11**, 4271–4277.

65 B. Liu, P. Xie, J. Zhao, J. Wang, M. Wang, Y. Jiang, J. Chang and X. Li, *Angew. Chem., Int. Ed.*, 2021, **60**, 8396–8400.

66 Y. Shi, Y. Qiao, P. Xie, M. Tian, X. Li, J. Chang and B. Liu, *Chin. Chem. Lett.*, 2024, **35**, 109544.

67 X. Xu, H. Shi, D.-H. Tan, P. Biallas, A. J. M. Farley, C. Genicot, K. Yamazaki and D. J. Dixon, *Chem. Catal.*, 2025, **5**, 101413.

68 T. Zhou, P.-F. Qian, J.-Y. Li, Y. B. Zhou, H.-C. Li, H.-Y. Chen and B.-F. Shi, *J. Am. Chem. Soc.*, 2021, **143**, 6810–6816.



69 C. M. B. Farr, A. M. Kazerouni, B. Park, C. D. Poff, J. Won, K. R. Sharp, M.-H. Baik and S. B. Blakey, *J. Am. Chem. Soc.*, 2020, **142**, 13996–14004.

70 C. Zhang, J. Jiang, X. Huang and J. Wang, *ACS Catal.*, 2023, **13**, 10468–10473.

71 Y.-Y. Liu, S. Cao, M.-P. Luo and S.-G. Wang, *CCS Chem.*, 2025, DOI: [10.31635/ccschem.025.202506179](https://doi.org/10.31635/ccschem.025.202506179).

72 Y. Zheng, J. Zhang, J. Bai, M. Wang and Z. Shi, *J. Am. Chem. Soc.*, 2025, **147**, 40833–40841.

73 W.-Q. Wu, P.-P. Xie, L.-Y. Wang, B.-B. Gou, Y. Lin, L.-W. Hu, C. Zheng, S.-L. You and H. Shi, *J. Am. Chem. Soc.*, 2024, **146**, 26630–26638.

74 Q. Zhou, B. Yang, G. Hao, M. Luo, S. Cao, B. Zhao, H. Yuan and S.-G. Wang, *Chin. J. Org. Chem.*, 2025, **45**, 2109–2120.

75 Y. Zheng, F. Xiang, J. Zhang, X. Yin, M. Wang and Z. Shi, *Angew. Chem., Int. Ed.*, 2025, e202519953.

76 P. W. Tan, A. M. Mak, M. B. Sullivan, D. J. Dixon and J. Seayad, *Angew. Chem., Int. Ed.*, 2017, **56**, 16550–16554.

77 S. Fukagawa, Y. Kato, R. Tanaka, M. Kojima, T. Yoshino and S. Matsunaga, *Angew. Chem., Int. Ed.*, 2019, **58**, 1153–1157.

78 D. Sekine, K. Ikeda, S. Fukagawa, M. Kojima, T. Yoshino and S. Matsunaga, *Organometallics*, 2019, **38**, 3921–3926.

79 L. Staronova, K. Yamazaki, X. Xu, H. Shi, F. M. Bickelhaupt, T. A. Hamlin and D. J. Dixon, *Angew. Chem., Int. Ed.*, 2024, **63**, e202316021.

80 S. Y. Hong, Y. Park, Y. Hwang, Y. B. Kim, M. H. Baik and S. Chang, *Science*, 2018, **359**, 1016–1021.

81 F. Schwizer, Y. Okamoto, T. Heinisch, Y. Gu, M. M. Pellizzoni, V. Lebrun, R. Reuter, V. Köhler, J. C. Lewis and T. R. Ward, *Chem. Rev.*, 2018, **118**, 142–231.

82 H. J. Davis and T. R. Ward, *ACS Cent. Sci.*, 2019, **5**, 1120–1136.

83 A. D. Liang, J. Serrano-Plana, R. L. Peterson and T. R. Ward, *Acc. Chem. Res.*, 2019, **52**, 585–595.

84 K. Yu, Z. Zou, N. V. Igareta, R. Tachibana, J. Bechter, V. Köhler, D. Chen and T. R. Ward, *J. Am. Chem. Soc.*, 2023, **145**, 16621–16629.

